

Precise Orbit Determination of Low Earth Orbiters with GPS Point Positioning

Sunil B. Bisnath and Richard B. Langley

*Geodetic Research Laboratory, Department of Geodesy and Geomatics Engineering,
University of New Brunswick, Fredericton, New Brunswick, Canada.*

BIOGRAPHIES

Sunil Bisnath received an Honours B.Sc. in 1993 and an M.Sc. in 1995 in Surveying Science from the University of Toronto. For the past five years he has been a Ph.D. candidate in the Department of Geodesy and Geomatics Engineering at the University of New Brunswick. During this time he has worked on a variety of GPS-related research and development projects, the majority of which have focused on the use of GPS for space applications.

Richard Langley is a professor in the Department of Geodesy and Geomatics Engineering at the University of New Brunswick, where he has been teaching and conducting research since 1981. He has a B.Sc. in applied physics from the University of Waterloo and a Ph.D. in experimental space science from York University, Toronto. Professor Langley has been active in the development of GPS error models since the early 1980s and is a contributing editor and columnist for GPS World magazine.

ABSTRACT

Precise orbit determination (POD) of low earth orbiters (LEOs) with GPS is becoming a standard practice in the space science community. The need for such information has been growing rapidly due to such scientific applications as radio occultation and ever increasing demands from engineering applications such as space-based earth sensor positioning. The conventional GPS-based POD strategies rely on data from a network of terrestrial GPS receivers as well as the spaceborne receiver. A complex, lengthy estimation procedure is carried out integrating the GPS data with high-fidelity dynamic models for the LEO. These strategies rely greatly on the GPS measurement strength, especially for low altitude spacecraft.

A completely geometric approach based on a kinematic, sequential least-squares filter/smoothers has been devised

by the authors which does not use dynamic models, but only data from the LEO's GPS receiver and the International GPS Service (IGS) GPS constellation precise ephemeris and clock data products. Since this approach makes no assumptions regarding receiver motion, it is platform independent. Preliminary static, terrestrial testing with nearly complete modelling of all associated error sources indicates that few decimetre position component r.m.s and few centimetre averaged position component bias are attainable. Initial spaceborne data testing produced sub-metre total displacement r.m.s. This result was however severely weakened by a low LEO receiver data rate. A number of processing and modelling enhancements will be introduced to refine this technique to allow for potential decimetre-level position component precision.

INTRODUCTION

Accurate, time-stamped locations of earth-orbiting satellites are required for a growing number of space missions and applications, ranging from satellite altimetry to atmospheric limb sounding, to synthetic aperture radar-based imaging. Traditional ground-based satellite tracking techniques are being supplemented or replaced by technologies such as GPS, where a spaceborne GPS (SGPS) receiver is placed aboard the satellite. Classical orbit determination (OD) techniques consisting of high-fidelity dynamic models utilize the GPS measurements to produce very precise orbits, *i.e.*, positions with decimetre or sub-decimetre Cartesian component precisions, in very complex OD strategies. See Bisnath and Langley [1999a] for descriptions and comparisons of these OD strategies. However, we contend that GPS alone may provide efficient and accuracy LEO orbits without recourse to dynamical modelling.

In the following sections a solely GPS-based orbit determination strategy – the geometric strategy – is described, a number of tests with terrestrial and

spaceborne data are discussed, conclusions are given, and plans for future research are specified.

GEOMETRIC ORBIT DETERMINATION STRATEGY

Classical OD was designed to incorporate sparse, often imprecise measurement data that are not necessarily three-dimensional in nature. The advent of SGPS has allowed for the direct collection of continuous, accurate, three-dimensional positions. Also, in mission scenarios involving low altitudes and irregularly-shaped spacecraft, the GPS measurements can potentially provide more accurate position estimates than the dynamics-based strategies.

Therefore a purely geometrical, GPS-based orbit determination strategy is proposed, utilizing only readily-available International GPS Service (IGS) data products (see, *e.g.*, Neilan *et al.* [1997]) and LEO receiver measurements. This provides for very efficient, straightforward processing and takes full advantage of the precise, three-dimensional and continuous nature of GPS measurements, as well as the existing GPS data infrastructure.

The processing flow of the strategy is shown in Figure 1. The input pseudorange and carrier-phase data are pre-processed to detect outliers, cycle slips, *etc.* and then used to form the processing observables. The LEO position is then estimated with the filter described in the following section. By applying an accurate interpolation procedure, LEO state estimates at non-GPS measurement epochs can also be determined producing the final orbit.

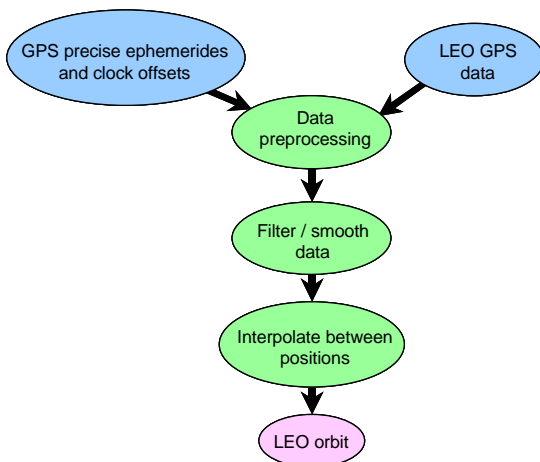


Figure 1: Processing flow of the geometric strategy.

Removal of Selective Availability

The original proposal of this strategy [Bisnath and Langley, 1999b] entailed the use of an array of static,

terrestrial reference receivers to be used to virtually eliminate GPS satellite and receiver clock offsets in a double-differenced, relative measurement scheme. This would have also required the use of IGS tropospheric zenith path delay estimates at the reference receivers. Simulations using this approach indicated that decimetre-level positioning in each LEO Cartesian component was possible [Bisnath and Langley, 1999b].

However, with the removal of Selective Availability (SA) from the GPS signal, precise GPS satellite clock information can be interpolated without fear of significant degradation. This eliminates the need for terrestrial reference receiver data and therefore double-differenced observables. The use of precise orbits and clocks can be viewed conceptually as the transfer of the terrestrial reference station position information to the GPS constellation. The result effectively is precise point positioning of the LEO receiver.

Phase-Connected, Point Positioning Filter Design

The use of only GPS measurements for satellite positioning can be achieved in a number of different ways ranging from pseudorange (code-phase) point positioning to some form of combined pseudorange and carrier-phase positioning. The latter approach is used in this strategy and its basic form can be attributed to the seminal work of Hatch [1982]. The crux of carrier and pseudorange combination is the use of averaged noisy code-phase range measurements to estimate the ambiguity term in the precise carrier-phase range measurements. The longer the pseudorange averaging, the better the carrier-phase ambiguity estimate.

The carrier/pseudorange averaging periods are typically short in spaceborne applications due to the relatively fast motion of the LEO, necessitating frequent changing of GPS satellites being tracked by the receiver. Such a situation does not allow for the highest precision of the technique to be attained. However by performing the averaging in the *position* rather than the *range* domain, previous position solutions can be used in estimating present and future position solutions. In essence, the pseudoranges provide coarse position estimates and the relative carrier phase measurements provide precise position change estimates. The position change estimates are used to map all of the position estimates to one epoch for averaging.

Similar processing filters have been described with a relative positioning formulation by several authors including Yunck *et al.* [1986] and Kleusberg [1986]. In fact, Yunck *et al.* proposed this type of filter in 1986 for the specific purpose of geometric GPS-based LEO orbit determination. However, this strategy was abandoned for others, since at the time a global array of terrestrial GPS

reference stations did not yet exist to provide sufficiently precise GPS ephemerides.

The observables fed to the filter are the ionosphere-free, undifferenced pseudorange and the ionosphere-free, time-differenced carrier-phase. For point positioning, a number of additional modelling considerations must be taken into account above and beyond those required for relative positioning (see *e.g.*, Zumberge *et al.* [1997] and Witchayangkoon [2000]). These include the relativistic GPS satellite clock correction due to the eccentricity in the satellite orbits; GPS satellite antenna phase centre to centre of mass offset; GPS satellite phase wind-up due to the relative rotation of the satellites with respect to the receiver; sub-diurnal variations in earth rotation; and consistency between the models used in the generation of the precise GPS orbits and clocks, and those used in the point positioning processing.

Given that this phase-connected, point positioning technique does not take into account the LEO dynamics nor makes any assumptions regarding dynamics, it can therefore be applied to any platform. This fact greatly enhances the utility of the approach and is used in our research for testing purposes. Note that GPS receivers in a terrestrial or airborne environment would be susceptible to additional systematic error sources which would need to be modelled, namely tropospheric effects in both situations and solid earth tides and ocean loading for terrestrial receivers.

Filter Models and Solution

The linearised filter observation model in matrix form is

$$\begin{bmatrix} \mathbf{P}_t - \mathbf{P}_t^0 \\ \mathbf{d}\Phi_t - \mathbf{d}\Phi_t^0 \end{bmatrix} = \begin{bmatrix} 0 & \mathbf{A}_t \\ -\mathbf{A}_{t-1} & \mathbf{A}_t \end{bmatrix} \begin{bmatrix} \mathbf{d}\mathbf{x}_{t-1} \\ \mathbf{d}\mathbf{x}_t \end{bmatrix} + \begin{bmatrix} \mathbf{e}_t \\ \mathbf{e}_{t-1,t} \end{bmatrix}; \quad (1)$$

$\mathbf{C}_{\mathbf{P}_t}, \mathbf{C}_{\mathbf{d}\Phi_t},$

where \mathbf{P}_t and \mathbf{P}_t^0 are the pseudorange measurement and predicted value, respectively; $\mathbf{d}\Phi_t$ and $\mathbf{d}\Phi_t^0$ are the time-differenced carrier phase measurement and predicted value, respectively; $\mathbf{d}\mathbf{x}_{t-1}$ and $\mathbf{d}\mathbf{x}_t$ are the estimated corrections to the LEO receiver position and clock at epoch t-1 and t, respectively; \mathbf{A}_{t-1} and \mathbf{A}_t are the measurement partial derivatives with respect to the LEO receiver position and clock estimates for epochs t-1 and t, respectively; \mathbf{e}_t and $\mathbf{e}_{t-1,t}$ are the measurement errors associated with \mathbf{P}_t and $\mathbf{d}\Phi_t$, respectively; and $\mathbf{C}_{\mathbf{P}_t}$ and $\mathbf{C}_{\mathbf{d}\Phi_t}$ are the covariance matrices for \mathbf{P}_t and $\mathbf{d}\Phi_t$, respectively. Note that at present the pseudorange and carrier phase measurements are assumed uncorrelated between observables and between observations.

The *best* solution for (1), in a least-squares sense, is

$$\begin{bmatrix} \hat{\mathbf{x}}_{t-1} \\ \hat{\mathbf{x}}_t \end{bmatrix} = \begin{bmatrix} \mathbf{x}_{t-1}^0 \\ \mathbf{x}_t^0 \end{bmatrix} - \begin{bmatrix} \mathbf{A}_{t-1}^T \mathbf{C}_{\mathbf{d}\Phi_t}^{-1} \mathbf{A}_{t-1} + \mathbf{C}_{\mathbf{x}_{t-1}}^{-1} & -\mathbf{A}_{t-1}^T \mathbf{C}_{\mathbf{d}\Phi_t}^{-1} \mathbf{A}_t \\ -\mathbf{A}_t^T \mathbf{C}_{\mathbf{d}\Phi_t}^{-1} \mathbf{A}_{t-1} & \mathbf{A}_t^T (\mathbf{C}_{\mathbf{P}_t}^{-1} + \mathbf{C}_{\mathbf{d}\Phi_t}^{-1}) \mathbf{A}_t \end{bmatrix}^{-1} \times \begin{bmatrix} -\mathbf{A}_{t-1}^T \mathbf{C}_{\mathbf{d}\Phi_t}^{-1} \mathbf{w}_{\mathbf{d}\Phi_t} \\ \mathbf{A}_t^T \mathbf{C}_{\mathbf{P}_t}^{-1} \mathbf{w}_{\mathbf{P}} + \mathbf{A}_t^T \mathbf{C}_{\mathbf{d}\Phi_t}^{-1} \mathbf{w}_{\mathbf{d}\Phi_t} \end{bmatrix}, \quad (2)$$

where $\hat{\mathbf{x}} = \mathbf{x}^0 + \mathbf{d}\mathbf{x}$ (the estimate is equal to the approximate initially assumed value plus the estimated correction); $\mathbf{w}_{\mathbf{P}}$ and $\mathbf{w}_{\mathbf{d}\Phi_t}$ are the misclosure vectors for the pseudoranges and time-differenced carrier phases, respectively; and $\mathbf{C}_{\mathbf{x}_{t-1}}^{-1}$ is the LEO receiver position and clock covariance based on the last epoch's observations.

As can be seen, the position estimate at the previous epoch, t-1, is used to estimate the position at epoch t and so on for the moving LEO. (2) represents a kinematic, sequential least-squares filter. This filter is a special case of the Kalman filter. Simply put, from (1) the pseudorange measurement contribution

$$\mathbf{P}_t - \mathbf{P}_t^0 = \mathbf{A}_t \mathbf{d}\mathbf{x}_t + \mathbf{e}_t; \quad (3)$$

$\mathbf{C}_{\mathbf{P}_t}$

can be extracted along with the carrier-phase measurement contribution

$$\mathbf{d}\Phi_t - \mathbf{d}\Phi_t^0 = -\mathbf{A}_{t-1} \mathbf{d}\mathbf{x}_{t-1} + \mathbf{A}_t \mathbf{d}\mathbf{x}_t + \mathbf{e}_{t-1,t}; \quad (4)$$

$\mathbf{C}_{\mathbf{d}\Phi_t}.$

The terms in (3) can be directly mapped to those of the Kalman filter measurement model, and with some rearrangement the terms in (4) can be effectively related to those of the Kalman dynamic model. That is, the kinematic, sequential least-squares tracking filter behaves like a Kalman filter because the carrier phase measurements represent its dynamic model. The filter process is illustrated in Figure 2.

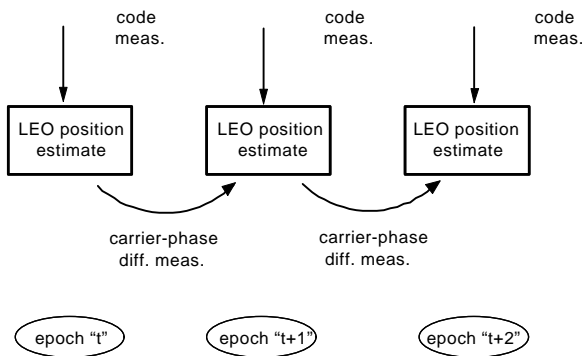


Figure 2: Combination of pseudorange and carrier-phase observations in the kinematic, sequential least squares filter.

Finally, since this tracking strategy is performed after-the-fact and not in real time, data smoothing can be performed. That is, the data arc can be processed in the forward and backward directions and the results can be optimally combined. The smoothed solution is

$$\hat{\mathbf{x}}_s = \mathbf{C}_f^{-1} \hat{\mathbf{x}}_f + \mathbf{C}_b^{-1} \hat{\mathbf{x}}_b, \quad (5)$$

where $\hat{\mathbf{x}}_s$ is the smoothed parameter estimate, \mathbf{C}_f is the forward filter parameter covariance, $\hat{\mathbf{x}}_f$ is the forward filter parameter estimate, \mathbf{C}_b is the backward filter parameter covariance, and $\hat{\mathbf{x}}_b$ is the backward filter parameter estimate [Gelb 1974]. This is a fixed-interval smoother in which the trace of the smoothed parameter covariance matrix is smaller than the trace of the covariance matrices of either filter.

PRELIMINARY TEST RESULTS AND ANALYSIS

In order to validate the geometric strategy a number of tests were conducted using the latest version of the developed processing software. This software is based on the University of New Brunswick's scientific GPS processing package DIPOP [Kleusberg *et al.*, 1993] and its components are not all completed, hence the preliminary testing. Where applicable, mention will be made of additional processing or modelling that is required.

Since the technique is platform-independent, the testing can be carried out not only on spaceborne data, but also on more prevalent terrestrial data. The results and analysis from two data sets are given here.

Static, Terrestrial Data Testing

The data used for this testing were collected over a one day period in August 2000 at Natural Resources Canada

(NRCan) station Algonquin (ALGO) in Ontario, Canada. The NRCan pre-processed TurboRogue receiver output contains dual-frequency code and carrier observables, with a 30 second sampling interval and a 5° elevation mask angle. The IGS precise GPS constellation orbit and clock product for the day was the only other input in the processing.

Since the troposphere is a significant contributor to the GPS error budget in this test, the UNB3 tropospheric prediction model (Collins [1999]) was used, but the residual delay was not estimated. This omission causes, on average, approximately decimetre-level biases in the position estimates. The receiver position and clock are estimated at the data sampling interval and this produces an error – a few centimetres at the most, arising from interpolating the 900 second interval IGS satellite clocks. The IGS has recently begun producing a separate 300 second interval GPS satellite clock product that will be used in future processing. Finally, ocean loading, earth orientation, and carrier phase wind-up have not been accounted for. These components can also produce centimetre-level errors in position, and will be modelled in the near future.

The objective of the testing with static terrestrial data was to investigate the repeatability of position computations with the technique and to test the performance of the technique against position results derived from double-difference, carrier-phase processing techniques by the international geodetic community.

The first aspect of the processing that was analysed, since this technique relies solely on GPS observations, was the geometric strength of the measurements used. Figure 3 contains the number of satellites tracked and the geometric dilution of precision (GDOP). As can be seen, there are always at least 5 satellites being tracked in this data set and in some cases up to 10. The average number for the processed data is 7.5. The GDOP typically remains between 2 and 4, but a few spikes exist where the number of tracked satellites goes down to 5. The average GDOP is 2.6. Given that there is a 5° elevation mask angle, these values are reasonable and represent geometrically strong measurements.

The results of the processing are presented in Figure 4. The error values are computed by differencing the estimated position from the benchmark International Earth Rotation Service (IERS), velocity-corrected, International Terrestrial Reference Frame 1997 (ITRF97) coordinates. The initialisation and convergence of the filter (thin blue lines) can be seen at the start of the time series. The smoothed results (bold green lines) are visually smoother than the filtered results. The spikes (especially in the vertical component) correspond well, as would be expected, to increases in the GDOP. And

finally, the error fluctuates the most in the vertical component. This as well is expected, given that the residual tropospheric delay was not estimated.

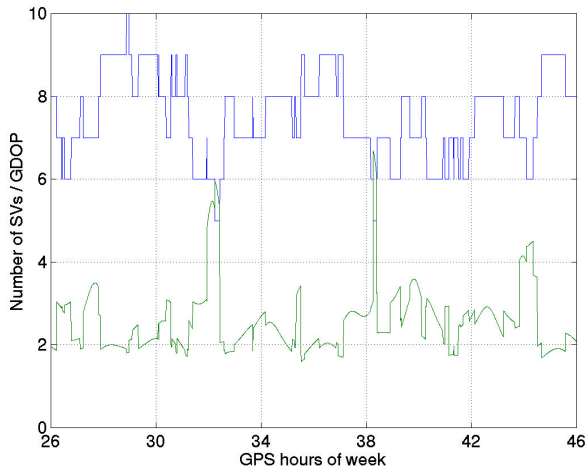


Figure 3: Number of Satellite Vehicles (SVs) and the Geometric Dilution of Precision (GDOP) for static, terrestrial data set.

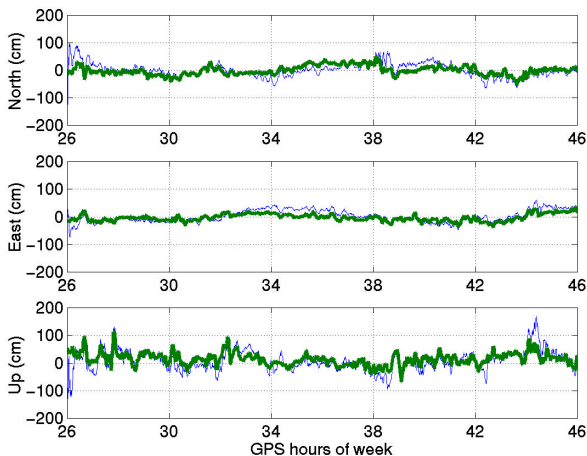


Figure 4: Component errors in position estimates for static, terrestrial data set. (Thin blue lines represent forward filter results, and bold green lines represent smoother results.)

Our qualitative comments are reinforced quantitatively with the summary statistics given in Table 1. The r.m.s. of the horizontal components of the filtered solution are between 22 and 25cm, while the vertical component is 37cm. Smoothing reduces the horizontal components to the 13 to 17cm level and the vertical component to the 27cm level. The smoothed total displacement r.m.s. is approximately 34cm.

r.m.s. (cm)	North	East	Up	Hori.	3-D
Filter	24.5	21.9	37.2	32.9	49.6
Smoother	16.8	13.3	26.7	21.4	34.2

Table 1: Summary statistics of component errors in position estimates for static, terrestrial data set.

The forward filter residuals are shown in Figure 5. The large initial phase difference values are due to filter initialisation. The pseudorange r.m.s. is 74cm with peak-to-peak variations of 10m and the phase difference r.m.s. is 2cm with peak-to-peak variations of 20cm. These values are larger than would be expected and are indicative of the errors not as yet modelled in the processing.

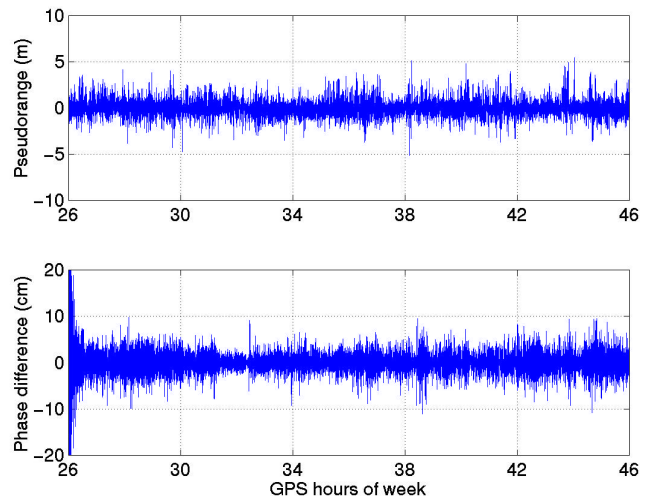


Figure 5: Forward filter observable residuals for static, terrestrial data set.

A final element of analysis that can be performed on this data set, since it represents static data, is to average the processed results. Again, the filter/smoothing makes no assumptions about the receiver's movements, so this averaging is done separately from the processing. The results from Figure 4 are re-plotted in Figure 6 in the form of a 3-dimensional scatter plot. The plot nicely illustrates the reduction in the outliers from smoothing (light green dots) as compared to the filtering (dark blue dots). However the smoothing causes an increase in the bias of the solution, as can be seen in Table 2. The filtered bias is approximately 1cm in each horizontal component and 7cm in the vertical component, while the total displacement bias is 7.5cm. The smoothed bias increases to 1 to 3cm in the horizontal and 14cm in the vertical. It is believed that this larger smoothed bias is due to a compounding of the initialisation biases existing in the

forward and backward filter runs. This can be removed by adjusting (tuning) the smoothing algorithm and modelling the remaining systematic effects.

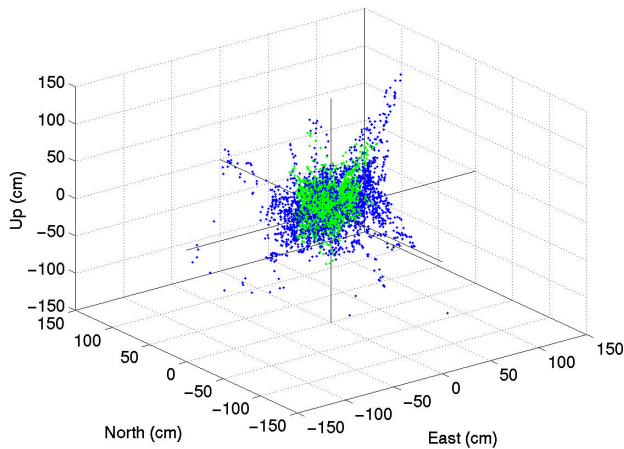


Figure 6: 3-dimensional scatter plot of component errors in position estimates for static, terrestrial data set. (Dark blue dots represent forward filter results, and light green dots represent smoother results.)

Bias (cm)	North	East	Up	Hori.	3-D
Filter	0.8	1.6	7.3	1.8	7.5
Smoother	-1.1	-3.5	13.7	3.7	14.2

Table 2: Summary statistics for averaged component errors in position estimates for static, terrestrial data set.

These preliminary static, terrestrial results indicate that decimetre-level spaceborne positioning results can potentially be achieved under certain conditions. We feel comfortable making this statement, since the largest error source that is not being accounted for in the terrestrial processing is the residual tropospheric delay, which is of no concern with spaceborne data. The only caveats are that there is similar measurement geometry and observable precision in the spaceborne measurements as in the terrestrial measurements.

Spaceborne Data Testing

The spaceborne data set consisted of one day of Topex/Poseidon data from November 2000. This LEO orbits at a nominal altitude of 1335km and provides single-frequency pseudorange and carrier-phase data. The data has been pre-processed at the Jet Propulsion Laboratory (JPL) to remove outliers, cycle slips and smooth the pseudoranges to provide observable data at

300 second intervals. No elevation mask angle was applied. The appropriate IGS precise GPS constellation orbit and clock offset file was the only additional input to the processing.

The purpose of this test was to investigate the geometric strength of the spaceborne measurements and to assess the practicality and performance of the technique against high-quality JPL orbits.

Figure 7 shows that the geometric strength of the available observations is significantly lower than that for the terrestrial data set we analysed. This is due in large part to the fact that this spaceborne receiver can only track a maximum of 6 GPS satellites and there are a large number of data gaps. The gaps exist in the JPL pre-processed data file and are increased by the primitive outlier detection in the UNB processing. The average number of satellites tracked is 5.4 and the average GDOP is 3.4. This represents an almost 50% reduction in the geometric strength of these measurements compared to the terrestrial measurements.

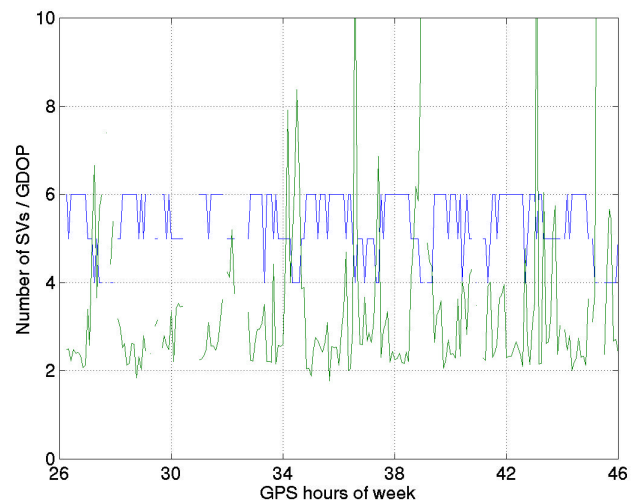


Figure 7: Number of Satellite Vehicles (SVs) and the Geometric Dilution of Precision (GDOP) for the Topex/Poseidon data set.

From this analysis it would appear that the conditions for potential decimetre-level positioning have not been met. The processing of these data also uncovered another measurement difficulty. The 300 second data sampling interval greatly reduced the number of time-differenced phase measurements because of the swiftly changing group of GPS satellites tracked by the receiver. The result of all these difficulties is a solution which contains many gaps and filter re-initialisations, which does not allow for proper filter convergence.

Figure 8 illustrates our results in the form of the total displacement error of the solution compared to the JPL orbit. The numerous gaps and filter re-initialisations (the hollow blue circles) are evident throughout the time series. A short period of continuous data that allowed for some filtering and smoothing was available between 34.5 and 36.5 hours. Since there is some error in the benchmark orbit, the following equation was used to take this error into account in determining the precision of the UNB results:

$$\text{rms}_{\text{unb}} = \sqrt{\text{rms}_{\text{total}}^2 + \text{rms}_{\text{jpl}}^2 - 2 \cdot \text{rms}_{\text{total}} \cdot \text{rms}_{\text{jpl}}} \quad (6)$$

Assuming no correlation between the errors in the JPL solution and the UNB solution, the filtered and smoothed UNB solutions would have r.m.s. errors of 107cm and 85cm, respectively. Assuming full correlation, the filtered and smoothed UNB solutions would have r.m.s. errors of 82cm and 63cm. It would be reasonable to assume that there is a significant amount of correlation, given that the same measurements were used to compute both solutions.

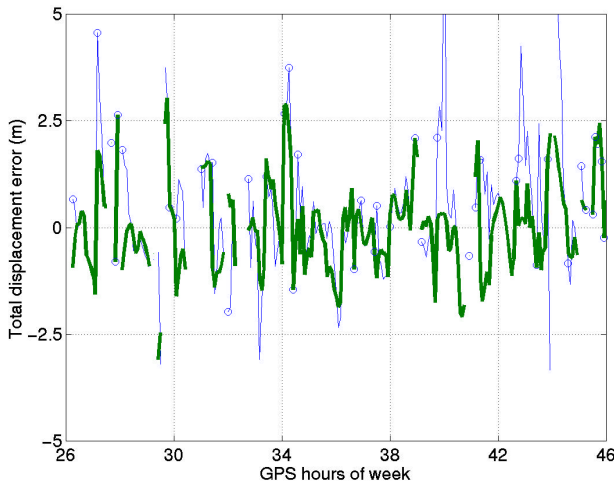


Figure 8: Total displacement errors in position estimates for Topex/Poseidon data set. (Thin blue lines represent forward filter results, bold green lines represent smoother results, and hollow blue circles represent pseudorange-only solutions.)

Figure 9 depicts the forward filter observable residuals. Again the data gaps can be clearly seen and are represented by straight lines connecting the residual values. The pseudorange r.m.s. is 95cm and the phase difference r.m.s. is 52cm. The time-differenced carrier-phase residuals remain large due to the short intervals of continuous data.

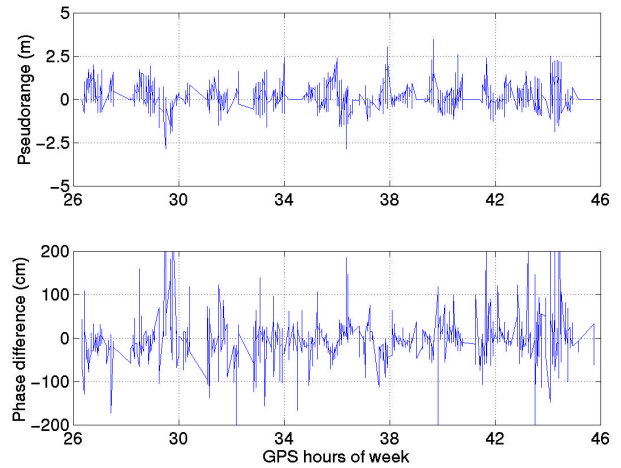


Figure 9: Forward filter observable residuals for Topex/Poseidon data set.

Even though these spaceborne results are not of as high a quality as the most precise orbits, the potential exists for great improvements. By processing the raw, high-rate Topex/Poseidon measurements, much of the geometric weakness will be remedied. Therefore much improved results are expected in future work.

INITIAL ORBIT INTERPOLATION STUDY

In order to utilize the discrete GPS-based position estimates in LEO mission applications, states may need to be accurately interpolated or approximated to epochs in-between these estimates. An initial investigation of the use of position interpolation was carried out.

Interpolation Methodology

Investigating the use of data interpolation, three parameters are of interest: the order of the interpolator, the spacing of the nodes of known functional values (in the case of the geometric strategy, position estimates spaced in time as dictated by the measurement sampling interval), and the accuracy to which the interpolation is to be carried out. The type of interpolator can have a significant effect on the results of the interpolator. For our study, a 15th order Lagrange interpolator was used.

A 24 hour, one second data set of the ERS2 satellite precise earth-centred, earth-fixed position estimates was used as a benchmark. ERS2 orbits at a nominal altitude of only 785km and therefore is significantly perturbed by the earth's gravity field. The position estimates were computed at the Delft University of Technology with satellite laser ranging (SLR) measurements, using the GEODYN II software package with all orbit perturbations turned on. Subsets of this data set were selected (depending on the node spacing), and processed with the interpolator. The results were then differenced with the

original data set to determine the accuracy of the interpolation process.

Interpolation Results and Analysis

The results for interpolation node spacing of 0 seconds to 180 seconds can be seen in Figure 10. The results have been represented in terms of the 99.7th percentile (3σ) interpolation error. That is, 0.3 percent of the errors are greater than or equal to the 3σ value. If the node interval is 90 seconds or less, no error is introduced in the LEO position solution due to interpolation. However, if an interval of 120 seconds is used, a small interpolator bias is introduced. Using a longer node interval would produce errors at a level equal to or greater than the resulting position noise from the above processing. The use of more sophisticated interpolation or approximation procedures might improve these results, but appropriate data sampling should allow for interpolation with negligible-error using our current procedure.

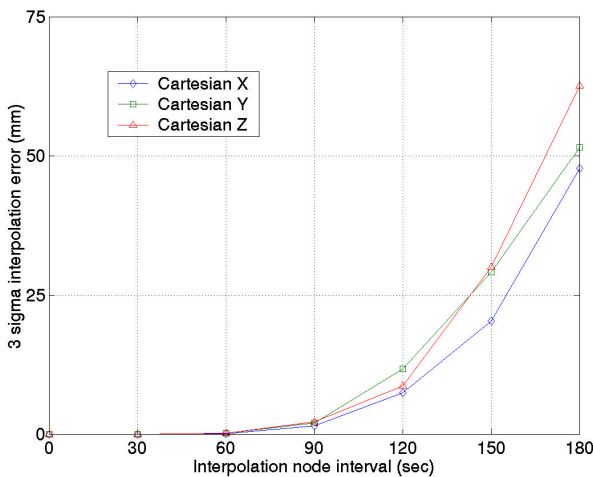


Figure 10: The effect of interpolation node interval on interpolation accuracy, for tests using ERS2 data.

CONCLUSIONS

An *a posteriori* LEO orbit determination strategy based solely on GPS measurements has been devised, which is simple and efficient. The strategy incorporates a kinematic, sequential least squares filter/smoothen that utilizes the full potential of the GPS measurements, and makes use of readily available GPS data products. As a by-product of the technique's design, its dynamics-free nature allows for it to be applied to any platform.

Static, terrestrial testing results indicate that few decimetre position component r.m.s. and few centimetre averaged position component bias are attainable. These

results are seen as promising as there are a number of improvements that have yet to be made in the processing. Preliminary spaceborne data testing indicates sub-metre total displacement r.m.s. is possible. While these results are sub-optimal, improved position estimates can be made for this data set using the high-rate raw data and adding additional pre-processing capabilities. Given all of our test results to date, the goal of decimetre-level position component precision is seen as attainable.

FURTHER RESEARCH

A number of processing and modelling capabilities are required to refine the present strategy and allow for the most accurate position estimates. The pre-processing will be expanded to robustly detect carrier-phase cycle slips and observable outliers. Modelling of earth rotation, phase wind-up and ocean loading will be included to account for these few-centimetre effects. Residual tropospheric estimation will be incorporated for terrestrial and airborne data processing. The so-called multipath divergence of the carrier-phase smoothed pseudorange will be mitigated through measurement de-weighting from multipath monitoring. And finally, it would be beneficial to produce a realistic, quantitative quality indicator of the state.

In terms of data processing, the static, terrestrial sample data sets will be re-processed with the additional functionality described. The high-rate Topex/Poseidon data will also be re-processed, as well as newly available CHAMP data. Finally, LEO position estimates will be re-computed using IGS high-rate GPS clock offsets and also predicted IGS GPS orbits.

ACKNOWLEDGEMENTS

Our research was conducted under a grant from the Natural Sciences and Engineering Research Council of Canada. The authors would like to thank Bruce Haines from the Jet Propulsion Laboratory for providing the Topex/Poseidon observables and ephemeris data, and Dennis Gerrits, visiting researcher from the Department of Aerospace Engineering, Delft University of Technology, The Netherlands for providing the ERS2 ephemeris data.

REFERENCES

- Bisnath, S.B. and R.B. Langley (1999a). "Precise *a posteriori* geometric tracking of Low Earth Orbiters with GPS." *Canadian Aeronautics and Space Journal*, Vol. 45, No. 3, pp. 245-252.
- Bisnath, S.B. and R.B. Langley (1999b). "Precise, efficient GPS-based geometric tracking of low earth orbiters." *Proceedings of the 55th Annual Meeting of the Institute of Navigation*, Institute of Navigation, 28-30 June, Cambridge, Mass., U.S.A., pp. 751-760.

- Collins, J.P. (1999). *Assessment and Development of a Tropospheric Delay Model for Aircraft Users of the Global Positioning System*. M.Sc.E. thesis, Department of Geodesy and Geomatics Engineering Technical Report No. 203, University of New Brunswick, Fredericton, New Brunswick, Canada, 174 pp.
- Gelb, A. (Ed.) (1974). *Applied Optimal Estimation*. Massachusetts Institute of Technology Press, Cambridge, Massachusetts, U.S.A., 374 pp.
- Hatch, R. (1982), "The synergism of GPS code and carrier measurements." *Proceedings of the Third International Geodetic Symposium on Satellite Doppler Positioning*, DMA, NOS, Las Cruces, New Mexico, 8-12 February, Physical Science Laboratory, New Mexico State University, Las Cruces, New Mexico, Vol. II, pp.1213-1232.
- Kleusberg, A., Y. Georgiadou, F. van den Heuvel, and P. Heroux (1993). "GPS Data Preprocessing with DIPOP 3.0," internal technical memorandum, Department of Surveying Engineering (now Department of Geodesy and Geomatics Engineering), University of New Brunswick, Fredericton, 84 pp.
- Kleusberg, A. (1986). "Kinematic relative positioning using GPS code and carrier beat phase observations," *Marine Geodesy*, Vol. 10, No. 3/4, pp. 257-274.
- Neilan, R.E., J.F. Zumberge, G. Beutler, and J. Kouba (1997). "The International GPS Service: A global resource for GPS applications and research." *Proceedings of the 10th International Technical Meeting of the Satellite Division of the Institute of Navigation*, Kansas City, Missouri, U.S.A., 16-19 September, 1997, The Institute of Navigation, Alexandria, Virginia, U.S.A., Vol. 1, pp. 883-889.
- Witchayangkoon, B. (2000). *Elements of GPS Precise Point Positioning*. Ph.D. dissertation, Department of Spatial Information Science and Engineering, University of Maine, Orono, Maine, U.S.A., 265 pp.
- Yunck, T. P., S.-C. Wu, and J.-T. Wu (1986). "Strategies for sub-decimeter satellite tracking with GPS," *Proceedings of IEEE Position, Location, and Navigation Symposium 1986*, Las Vegas, Nevada, U.S.A., 4-7 November, The Institute of Electrical and Electronics Engineers, Inc., New York, New York, U.S.A., pp. 122-128.
- Zumberge, J.F., M.B. Heflin, D.C. Jefferson, M.M. Watkins, and F.H. Webb (1997). "Precise point positioning for the efficient and robust analysis of GPS data from large networks." *Journal of Geophysical Research*, Vol. 102, No. B3, pp. 5005-5017.